TESLA-Report 1994-03

Detailed Studies of Anomalous Loss Mechanisms in S.C. 3GHz Single-cell Cavities at E_{peak} up to 70MV/m and Q_0 up to $7 \cdot 10^{10}$

D.Reschke, W.Görlich, G.Müller, H.Piel, J.Pouryamout, R.W.Röth
Fachbereich Physik, Bergische Universität Wuppertal, Germany

ABSTRACT

Although the main limitation of today's s.c. niobium accelerator cavities is field emission, the best experiments show thermal breakdown and residual resistance as the next limits for gradients above 20 MV/m. We report on a series of 12 experiments on four 3GHz single-cell niobium cavities (RRR = 200 - 1000), investigating these effects in detail. After standard preparations at CEN Saclay (BCP) and at Wuppertal University (BCP, firing), surface fields E_{peak} above 50 MV/m and quality factors Q_0 above 10^{10} are achieved with good reliability. The influence of the residual gas composition in the vacuum system of the cavity on both, the residual resistance and field emission is investigated. Hydrocarbons are identified as the origin of a strong degradation of the cavity performance. In addition, the effect of the exposure to various gases ($p \approx$ mbar) at room temperature is studied. Detector systems for x-ray mapping and thermometry in superfluid helium are essential for a locally resolved, quantitative analysis of the various loss mechanisms.

INTRODUCTION

For a superconducting linear accelerator in the TeV-regime (TESLA) acceleration gradients E_{acc} above 20 MV/m at quality factors of $> 5 \cdot 10^9$ are required [1]. Despite the progress in suppression of field emission and the increase of the thermal breakdown field, such values are achieved today only in laboratory experiments, but not in real accelerator operation. Although high purity niobium (RRR ≥ 300) and postpurification techniques are used, the limitation by thermal breakdown at local defects occurs again at $H_S = 110 - 135$ mT ($\triangleq E_{acc} = 25 - 30$ MV/m) [2,3,4]. To provide thermal stability at such high fields [5] and to allow for acceptable cryogenic costs, the residual surface resistance must be very small, especially for frequencies above 1 GHz. In addition, the thermal conductivity λ has to be increased further [6] and the density of local defects must be reduced.

Though the cleaning and assembling techniques were significantly improved during the last years, the residual resistance is not well under control and varies, even in "successful" experiments, about one order of magnitude (typical: $Q_0 = 5 \cdot 10^9 - 5 \cdot 10^{10}$). Moreover, a drop of Q_0 with increasing field amplitude, which is not due to field emission, is often observed and needs, as well as residual resistance at low field, a better understanding.

MATERIAL, PREPARATION AND EXPERIMENTAL SETUP

The material of the four 3GHz single-cell cavities reflect impressively the improvement of the available high purity niobium (Nb). The cavities SW1 and SW2 were fabricated from Heraeus sheet Nb with RRR = 135 and RRR = 90, respectively. After postpurification with the well-known solid state gettering with titanium [7,8] the RRR increased to 250 - 300. The cavity SW5 was fabricated from russian Giredmet sheet Nb of RRR = 500, which improved to RRR ≈ 1500 after double-sided titanisation. The half-cells of cavity SW6 were machined of bulk Nb (RRR = 800) at IHEP Protvino and e-beam welded at Leybold,USA. An overview of the cavity parameters is given in Table 1.

Table1: Cavity parameters

Cavity	RRR (as fabricated)	RRR (postpurified)	G [Ω]	$\frac{E_{peak}}{E_{acc}}$	$\frac{H_{peak}}{E_{acc}}\left[\frac{mT}{MV/m}\right]$
SW1	135	~280	290	2.55	4.18
SW2	90	~260	"	"	"
SW5	500	≤1500	"	"	"
SW6	800	–	246	2.0	4.4

In the course of the 12 experiments three different preparation techniques were applied:

1) Standard open chemical treatment (BCP) + High temperature annealing at 1000°C (HTA) + Dry dustfree assembly (Class 10-100) → 3 Tests

2) Standard open chemical treatment + Ultrapure water rinsing (2ℓ/min) + (partially: Drying with pure N_2) + Dustfree assembly (Class 10-100) → 6 Tests (3 treatments at CEN Saclay, 3 treatments at Wuppertal)

3) Only HNO_3 rinsing + Ultrapure water rinsing (2ℓ/min) + Dustfree assembly (Class 10-100) → 2 Tests

One experiment was done after breaking the vacuum under cleanroom conditions and dustfree reassembling. Room temperature cycles or gas exposure at room temperature are not counted as separate experiments.

RF- and He-processing has been done up to 40 W in cw and long pulse (>10ms) operation. A rotatable, high resolution thermometry system with 13 Stycast-isolated "thermometers" has been used to detect the temperature distribution of the RF-losses in superfluid helium. In addition, the rotatable frame includes 15 X-ray detectors to detect the local distribution of the Bremsstrahlung in case of field emission. A detailed quantitative analysis of the located defects and emitters was partially performed in a reproduction test, where the thermometers are glued with Apiezon N grease to the spots of highest interest. With a quadrupol mass spectrometer the composition of the residual gas in the vacuum system is controlled before and during the RF-tests.

RF-RESULTS

The RF-results of the 12 experiments are summarized in Table 2.

Although we have only a relatively small number of experiments, several nice results can be derived from the data:

- The applied surface treatments result with a high reproducibility in electrical peak surface fields above 50 MV/m (≙ E_{acc} > 20MV/m) and Q-values above 10^{10} (Fig.1, 2).
- The diagnostic systems identified clearly two accidents during fabrication (SW6-2: bad welding) and preparation (SW5-9: contaminated vacuum system), respectively.
- Field emission started (excluding the accidents) beyond E_{peak} > 30MV/m. The field emission onset of the best experiment reached nearly 70MV/m after a preparation at Saclay.

- There is a trend that N_2-drying after BCP and ultrapure water rinsing leads to improved residual Q-values compared to an open drying under cleanroom conditions. The best value of $Q_0 = 7 \cdot 10^{10}$ (Fig.1) corresponds to a residual surface resistance $R_S = 4.1\,n\Omega$. This is very close to the sum of the BCS surface resistance $R_{s,BCS} \approx 2\,n\Omega$ at 1.4K and the surface resistance due to frozen-in-flux of the remaining magnetic field in the cryostat $R_{s,fif} \leq 4n\Omega$.
- A "soft" surface treatment with only a HNO_3 soak + ultrapure water rinsing was used after test SW2-18 to preserve the successfully tested surface before a complete new assembling of the cavity. Contrary to our expectation, both experiments (SW2-19, SW2-20) resulted in an increased residual surface resistance. Even if this degradation was not caused by the first treatment, the second preparation was not sufficient to remove this kind of contamination. Thus the applied "soft" surface treatment is inadequate aiming for a reproducable high cavity performance.
- As expected for the high RRR niobium material, cavities SW1, SW2 and SW5 achieve magnetic surface fields above 100 mT without a local thermal breakdown.
- Nearly all degradations of the $Q(E_{acc})$-performance (especially SW1-20-I, SW5-10-I, SW5-11) occured during field emission or processing of field emission. (Remark: For clearness the table does not contain all intermediate states during field emission and processing of field emission.)
- The cavity performance usually did not change after a room temperature cycle, even if the test set-up was moved by crane. This indicates, that there are no loose particles at the top flanges "snowing" into the cavity.
- The influence of the composition of the cavity vacuum and of the exposure to various gases is discussed in the next chapter.

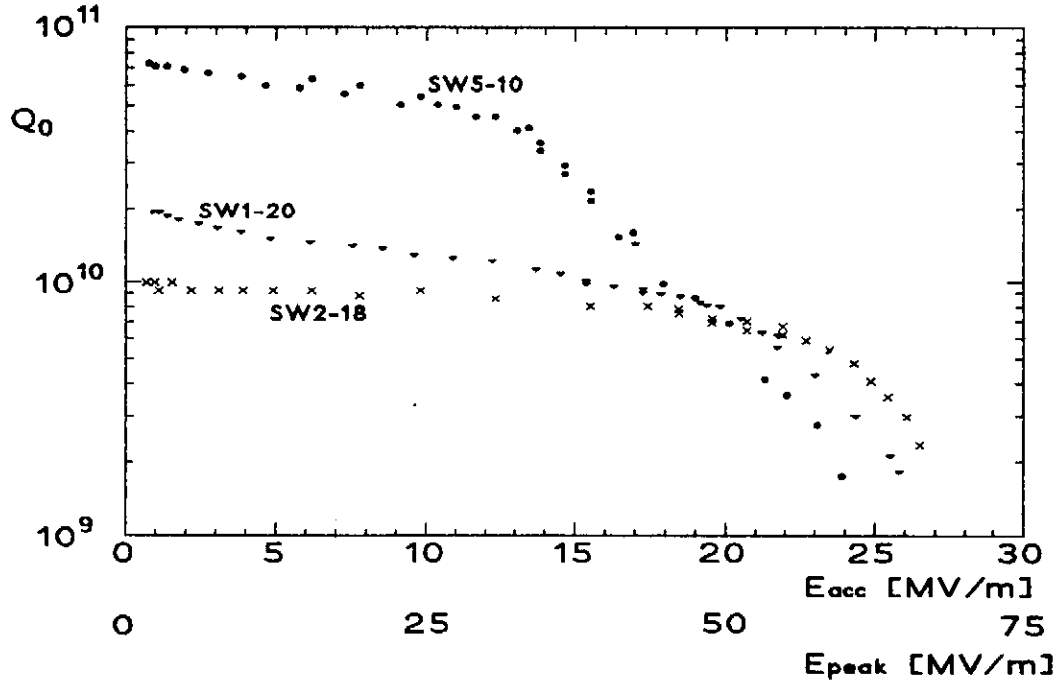

Fig.1: Typical $Q(E_{acc})$-performances of 3 tests (see Table2)

For 3 experiments we had the opportunity to use the infrastructure at the CEN Saclay for the surface treatment of the cavities SW2 and SW5. The first preparation (SW2-18) included an "open" BCP and an "open" ultrapure water rinsing in the class 10 area of the cleanroom. After drying under laminar air flow the cavity was closed with teflon hats and transported to the cleanroom in Wuppertal, where the final assembly was performed. The second and third preparation (SW2-21, SW5-11) also started with an "open" BCP. Differently to the first preparation, both cavities were water rinsed and dried using the closed-cycle integrated chemical facility [10]. While SW5 was assembled in the cleanroom at Saclay, SW2 was again transported to Wuppertal with Teflon flanges. Both tests of SW2 showed the highest measured fields ($E_{peak} \approx 70$MV/m), clearly demonstrating that a careful transport under clean conditions does not lead to a degradation of the cavity performance for gradients up to $E_{acc} \approx 25$MV/m.

All RF results listed in Tab.1 are obtained at a temperature of about T = 1.4K. Above 1GHz and at T ≈ 2K, which are the operation parameters of accelerators like CEBAF and TESLA, the RF losses are increased or dominated by the BCS contribution to the surface resistance. Furthermore, the Kapitza resistance, which hinders the transport of heat from the Nb wall to the He-bath, depends inversely with a high power law on the He-bath temperature. Both effects might result in different thermal breakdown conditions at 1.4K and 2K. However model calculations predict for the temperature range of T = 1.4K to T = 2.1K and local defects up to 100µm spot size a nearly constant magnetic breakdown field [6] at frequencies $f_0 \leq 3$GHz. Therefore in five of the best experiments the $Q(E_{acc})$-performance was determined also at 2.0 - 2.1K. In good agreement with the model calculations the "quench" limited test SW2-18 provided at T = 2.1K ($H_{peak} = 104.1$mT) and T = 1.4K ($H_{peak} = 110.8$mT) a nearly constant breakdown field. The same behaviour was observed at a 3GHz nine-cell structure [9], limited by a local thermal breakdown at $H_{peak} = 74.5$ mT. Moreover the field emission limited experiments showed no contradiction to these results at H_{peak} of at least 90 mT, so that magnetic surface fields of about 100 mT at T = 2K and $f_0 \leq 3$GHz can be achieved reproducibly in postpurified niobium.

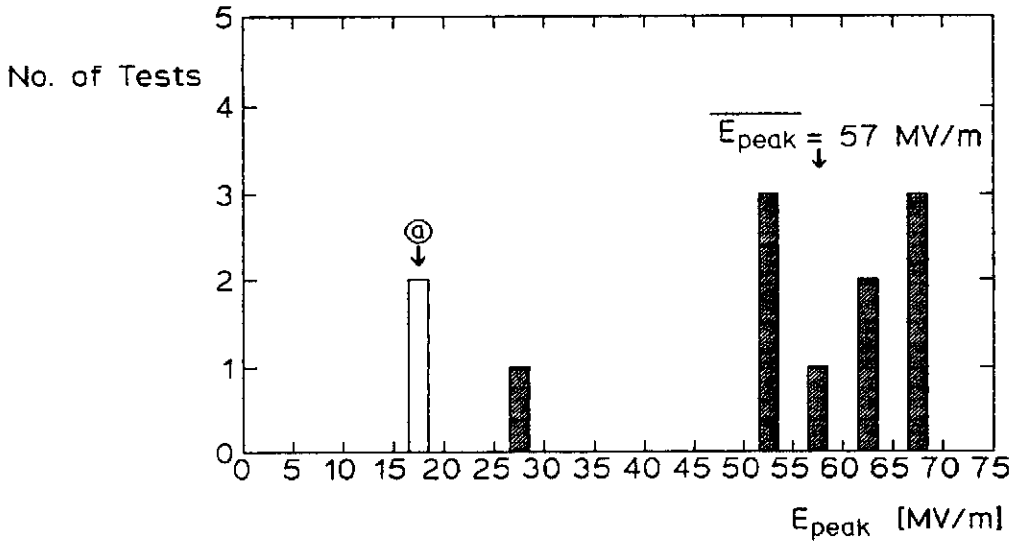

Fig.2: Maximum electric peak fields of the 12 experiments. The worst results (ⓐ) are due to test SW5-9 with contaminated vacuum and test SW6-2 with a bad welding.

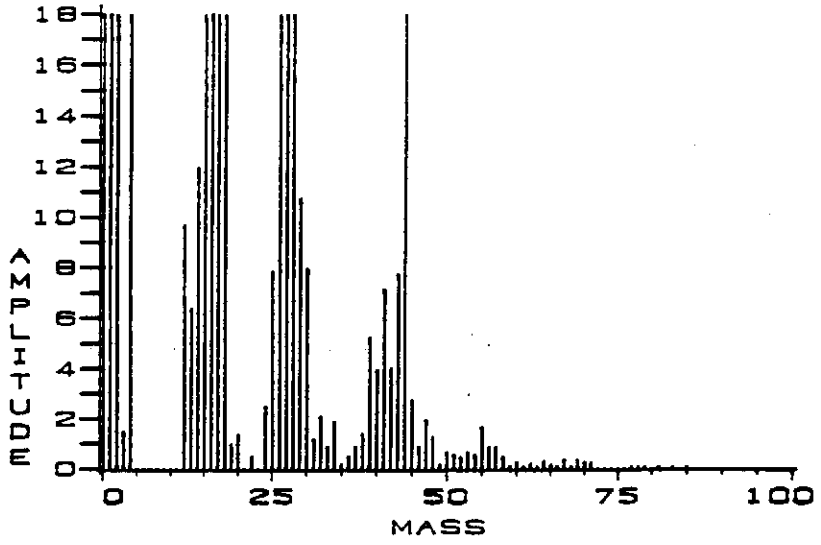

Fig.3a: Mass spectrum of the contaminated vacuum system during test SW5-9

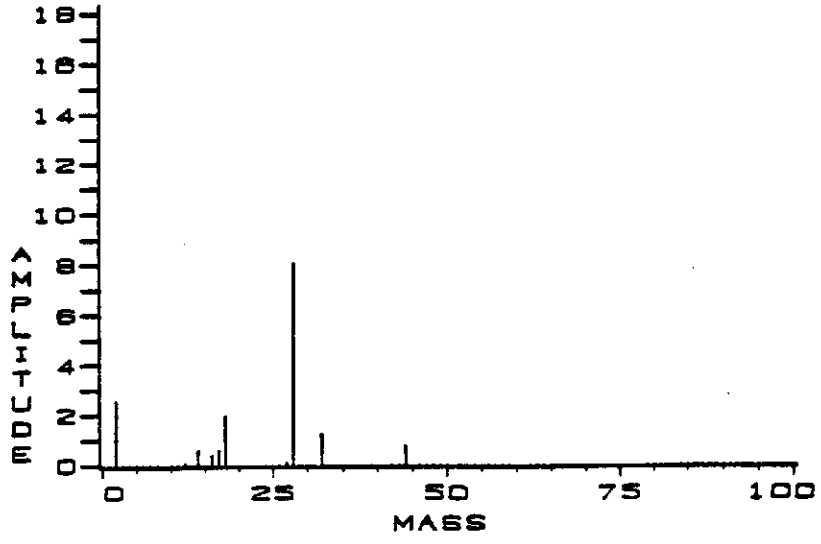

Fig.3b: Mass spectrum of the vacuum system during SW5-10

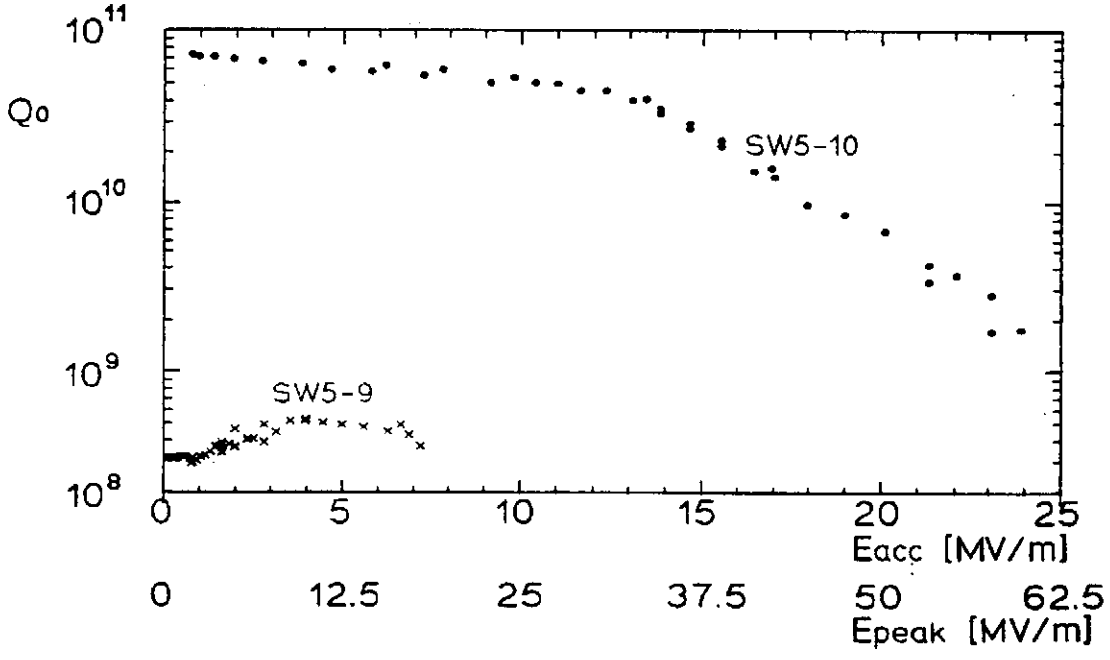

Fig.3c: $Q(E_{acc})$-curves before (SW5-9) and after (SW5-10) curing the hydrocarbon contamination

INFLUENCE OF CAVITY VACUUM AND VARIOUS GASES ON THE $Q(E_{acc})$-PERFORMANCE

It is well known, that a bad cavity vacuum usually results in a poor RF-performance. Furthermore it is obvious, that the composition of the residual gas rather than the total pressure is the dominating factor. An involuntary example is given by test SW5-9. Though the total pressure of the cavity vacuum was in the order of 10^{-7}mbar, the mass spectrum analysis (Fig.3a) shows clear evidence for a contamination by hydrocarbons (Mass 39, 41, 43, 50 - 57 and higher). The following cryotest exhibited the worst RF performance of the experimental series with a Q-value of $6 \cdot 10^8$ and field emission starting at $E_{peak} = 15.6$MV/m (Fig.3c) Cleaning and baking of the vacuum components together with the use of an oilfree turbo pump resulted in mass spectra (Fig.3b) free of hydrocarbons related with the best measured Q-value of $7 \cdot 10^{10}$ and a field emission onset of $E_{peak} = 39.5$ MV/m (Fig.3c).

Together with a number of former experiments, the source of the hydrocarbon contamination has been identified most probably as the oil of the vacuum pumps. Most critical parts are the bellows near to the cavity, which easily accumulate existing contaminations, but are difficult to clean. Thus the use of oil-free vacuum pumps, regular baking of the vacuum system and permanent control with a mass spectrometer are of highest importance aiming for a low residual surface resistance and a high field emission threshold.

Beside contaminations like hydrocarbons, we have studied the influence of "regular" gases like air, N_2, He, CO_2 etc. with respect to residual resistance and field emission. Though the effect of adsorbed gases on the cavity performance was reported in a number of publications [11,12,13,14], these results of various laboratories differ and are partially contradictory.

During the experiment SW1-20-i (Fig.1) the cavity was warmed up to room temperature between the cryotests and exposed to He, N_2, synthetic air and CO_2 with a pressure of a few millibar. After evacuation the next cryotest was performed. Over the seven tests the residual Q-value degraded from $Q_0 = 3.5 \cdot 10^{10}$ to $Q_0 = 1.4 \cdot 10^{10}$ including the four gas exposures and two times removal and assembly of the test insert to the cryostat. As mentioned above, the irreversible degradations of the residual Q-value occured mainly during field emission or its processing. Only the removal of the test set-up from the cryostat between SW1-20-4 and SW1-20-5 resulted in a degradation of $Q_0 = 1.9 \cdot 10^{10}$ to $Q_0 = 1.4 \cdot 10^{10}$. However, the exposure of the cavity to the four gases did not show any significant and lasting influence on the residual Q-value. Especially the exposure to CO_2, which was reported to cause a strong degradation [12], resulted in an unchanged Q-value, even in the case of an additional gas exposure at 1.5K. No correlation of the field emission activity to the gas exposures was found. The onset field varied during the series between $E_{peak} = 34$MV/m and $E_{peak} = 44$MV/m. The lowest values were observed in test SW1-20-5 and SW1-20-6 after the second removal of the test set-up from the cryostat (see above). As can be seen clearly on the x-ray maps at $E_{peak} = (51 - 59)$ MV/m (Fig.4), the location of the emission varies from test to test as well as during one test (SW1-20-2). According to trajectory calculations, most of the primary electrons hit the surface close to the emitter, producing the narrow peaks. The scattered and more energetic secondary electrons are responsible for the broad x-ray peaks at the opposite iris. Remarkable is the nearly homogenous underground over all angle positions. The x-ray maps show 2-3 field emitters, which are activated alternately at nearly the same threshold. These emitters could not be destroyed with RF- and He-processing. The field enhancement factor β was determined for all $Q_0(E_{acc})$-runs using the current of free electrons measured at the transmitted power probe. The initial β-factors before processing vary between 120 and 145, which are lowered to values between 60 to 90 after processing.

This series and, in addition, the reassembly of cavity SW2 in the cleanroom (SW2-16 → SW2-17) gave no indication of a degradation of the $Q_0(E_{acc})$-behaviour due to the exposure to gases like air, N_2, He and CO_2. Of course, it is a must to use pure, filtered gases as well as clean installations and a careful operation. Fulfilling these requirements, even on a level of residual Q_0-values above 10^{10} and surface fields of 50-70MV/m the cavity vacuum can be broken, the cavity can be transported and finally reassembled without any degradation of its performance.

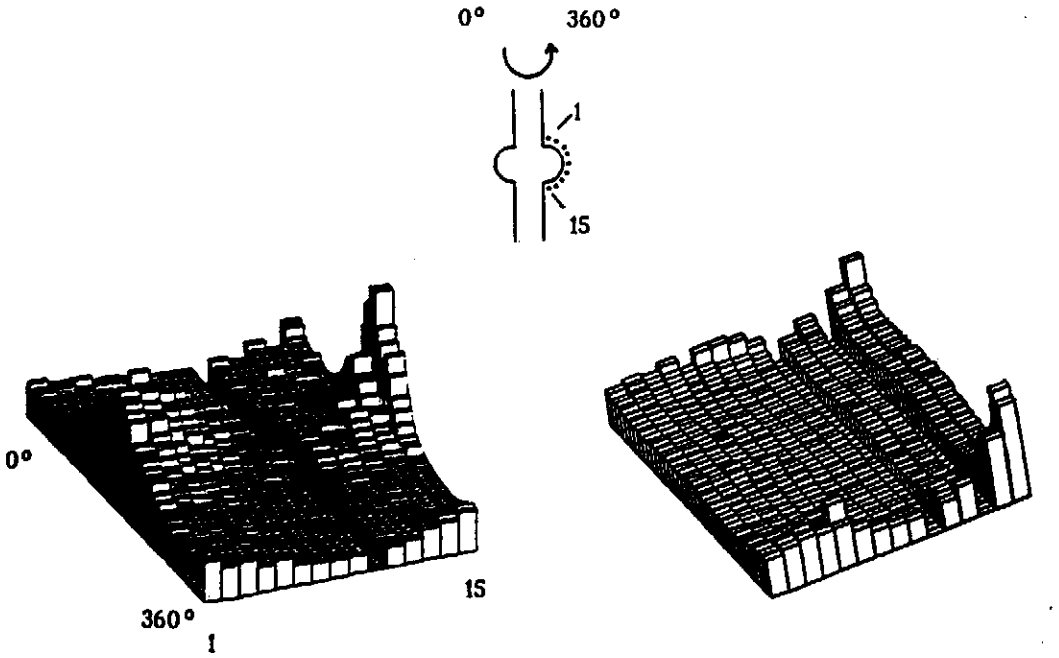

SW1-20-1, E_{acc}=21 MV/m

SW1-20-2, E_{acc}=23 MV/m

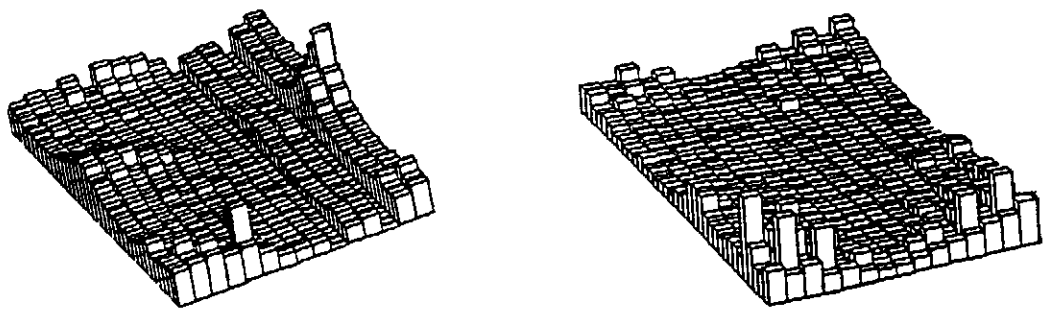

SW1-20-2, E_{acc}= 20 MV/m

SW1-20-4, E_{acc}= 22 MV/m

Fig.4: X-ray maps taken during experiment SW1-20-1 to SW1-20-4 (E_{peak}=(51-59)MV/m).

LOCAL DISTRIBUTION AND FIELD DEPENDENCE OF THE RESIDUAL SURFACE RESISTANCE

Quantitative information about the local distribution and the field dependence of the residual surface resistance can be obtained with thermometry in superfluid helium [15,16]. At first, temperature maps with complete spatial resolution are measured with a set of scanning thermometers detecting local defects and temperature increases due to electron bombardement in case of field emission. In a second cryotest the thermometers are glued to the cavity wall with Apiezon N grease for a quantitative analysis:

$$\Delta T = \eta(T_{out}) \cdot R_K(T_{bath}) \cdot \left(dP/dA \right)^{\alpha} \qquad (1)$$

where

$$dP/dA = 1/2 \cdot R_s^{loc}(T_{in}) \cdot H_s^{\ loc\,2} \qquad (2)$$

T_{in} and T_{out} are the temperatures at the inner side and the outer side of the cavity wall, respectively, with $T_{out} = T_{bath} + \Delta T$. The exponent α is in good agreement with 1 [17]. The Kapitza resistance depends on the bath temperature with strong power law $R_K \sim T_{bath}^{-3} - T_{bath}^{-5}$ in various literature data [16].

In the case of negligible local heating due to field emission, one obtains:

$$\Delta T = 1/2 \cdot \eta(T_{out}) \cdot R_K(T_{bath}) \cdot R_s^{loc}(T_{in}) \cdot H_s^{loc\,2} \qquad (3)$$

The efficiency $\eta(T_{out})$ varies significantly from test to test for each single thermometer due to the varying thermal contact of the thermometers to the cavity wall. This behaviour results in a different insolation against the superfluid helium with its extremly high thermal conductivity. Thus, it is not sufficient to use the data of a former calibration measurement [17] as it was practiced in a first experiment determining the local surface resistance using the temperature increase on the cavity wall [11].

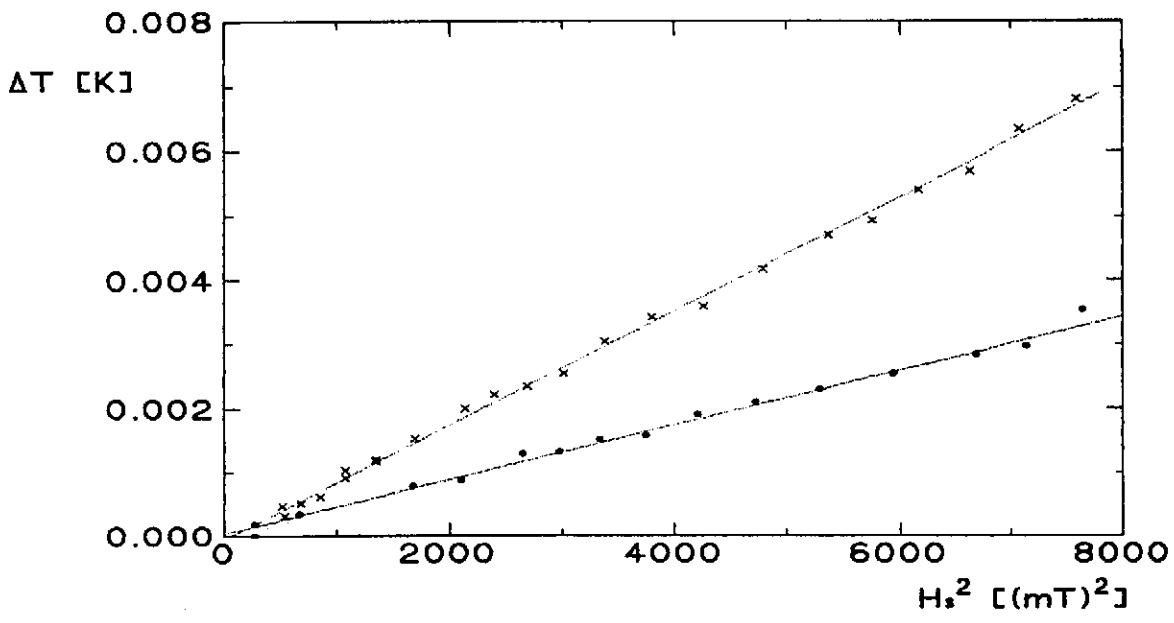

Fig.5: ΔT versus H_s^2 of two thermometers at the equator used for the calibration of η
As expected at 2K, the BCS surface resistance is dominating and results in $\Delta T \sim H_s^2$

At our operation frequency $f_0 \approx 3$ GHz and a bath temperature of $T_{bath} = (2.0-2.1)$K the BCS surface resistance $R_{s,BCS}$ is in the order of $(50-100)\,n\Omega$ and thus large compared to the residual resistance $R_{s,res}$, which is usually less than $10\,n\Omega$ ($\triangleq Q_{0,res} \geq 10^{10}$). Therefore at $T_{bath} = (2.0-2.1)$K a well defined temperature increase ΔT is observed on the whole cavity wall (Fig.5). The slope of the measured ΔT vers. H^2 can be analysed with respect to η for each thermometer and result in typical η-values of 0.05-0.1. Obviously, this holds only below the field emission threshold. Nevertheless the scaling of η from $T_{bath} \approx 2$K to $T_{bath} \approx 1.4$K yields in an error of about 20% due to observed variations of the scaling law for different assembled thermometers [16]. At $T_{bath} = 1.4$K the η-values for thermometers, which are in good contact to the cavity wall, vary between 0.4 and 0.9.

In addition for precise measurements, both, at $T_{bath} \approx 2$K and at $T_{bath} \approx 1.4$K, it is of great importance to correct the measured ΔT-values with respect to the bath temperature increase during the read-out time of the chain of thermometers. Especially at high fields, the RF-power deposited in the cavity wall heats the helium bath significantly during the read-out time, which lasts typically for a few seconds. Therefore, the bath temperature is detected by an additional thermometer.

Five experiments, including the elsewhere reported first one [11], are analysed in detail. Three cases can be distinguished:

- Limitation due to a local thermal breakdown at a detected defect ; $Q_{0,res} \approx 10^{10}$ (2 Tests)
- No detected defect ; Limitation due to field emission ; $Q_{0,res} > 2 \cdot 10^{10}$ (2 Tests)
- Detected defect <u>without</u> local thermal breakdown ; Limitation due to field emission ; High residual resistance $R_{s,res} = 58\,n\Omega \triangleq Q_{0,res} = 5 \cdot 10^9$ (1 Test)

Local thermal breakdown

In a first cryotest, the defect responsible for the "quench" was located and identified near the equator. In the second cryotest with fixed thermometers, the temperature of the cavity wall close to this defect was found to increase nearly exponentially with the magnetic surface field (Fig.6a). This result cannot be explained by simple thermal model calculations with constant defect resistance and without taking the presence of the thermometer into account, which predict a temperature increase $\Delta T \sim H^2$ (Fig.6b) [6].

In experiment SW2-18-1 the defect-free areas near to the equator show the predicted temperature increase $\Delta T \sim H^2$ (Fig.7). A least-square fit to the data of various thermometers up to the field emission threshold of $E_{acc} \approx 20$MV/m give a local surface resistance of $R_{s,loc}(1.4K) = (3-8)\,n\Omega$. This value is quite close to the sum of the BCS surface resistance $R_{s,BCS}(1.4K) \approx 2.5\,n\Omega$ and the surface resistance due to frozen-in-flux of the remaining magnetic field in the cryostat $R_{s,fif} \leq 4\,n\Omega$. Thus, most of the cavity surface shows a magnetically caused low residual surface resistance, which is at least one order of magnitude less than the value determined by the RF-measurement ($R_{s,res} = 31\,n\Omega$). A similiar result was obtained in the first experiment. Therefore not only the "quench", but most of the residual resistance and the observed increase of $\Delta R_S \sim H_s^2$ (Fig.6c) has to be attributed to the local defect.

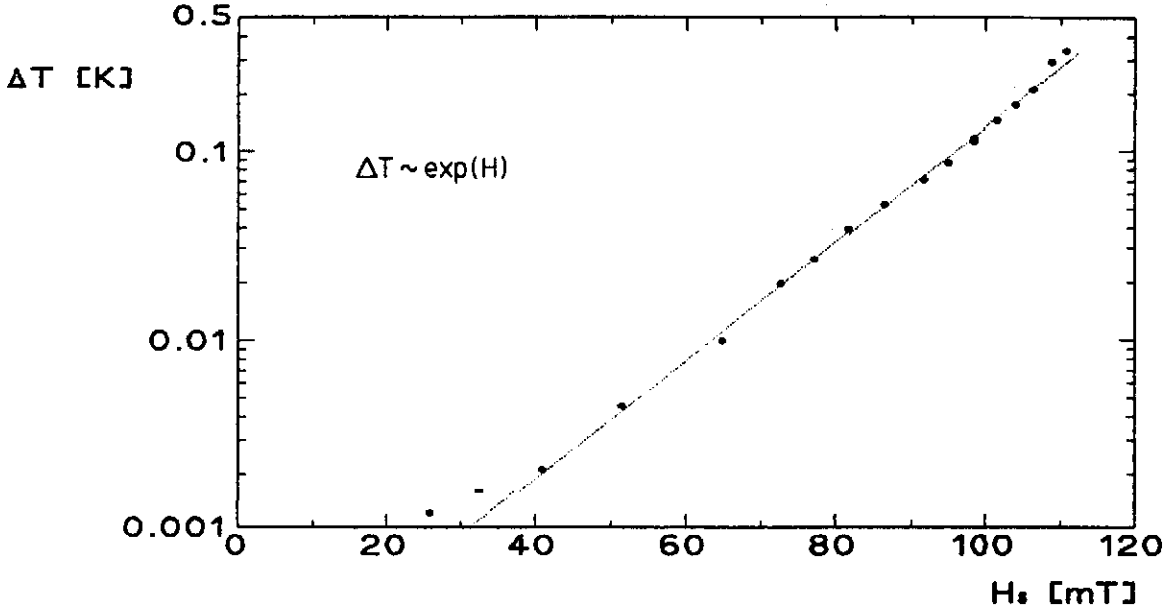

Fig. 6a: Measured field dependence of the temperature increase at the local defect (SW2-18-1)

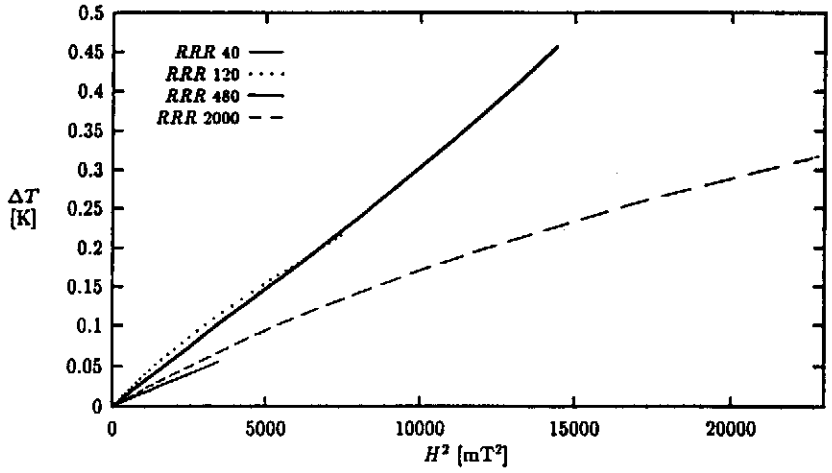

Fig. 6b: Calculated field dependence of the temperature increase at the local defect (R_D =8mΩ, r_D = 10μm, T_B = 1.4K). The parameter is the RRR.

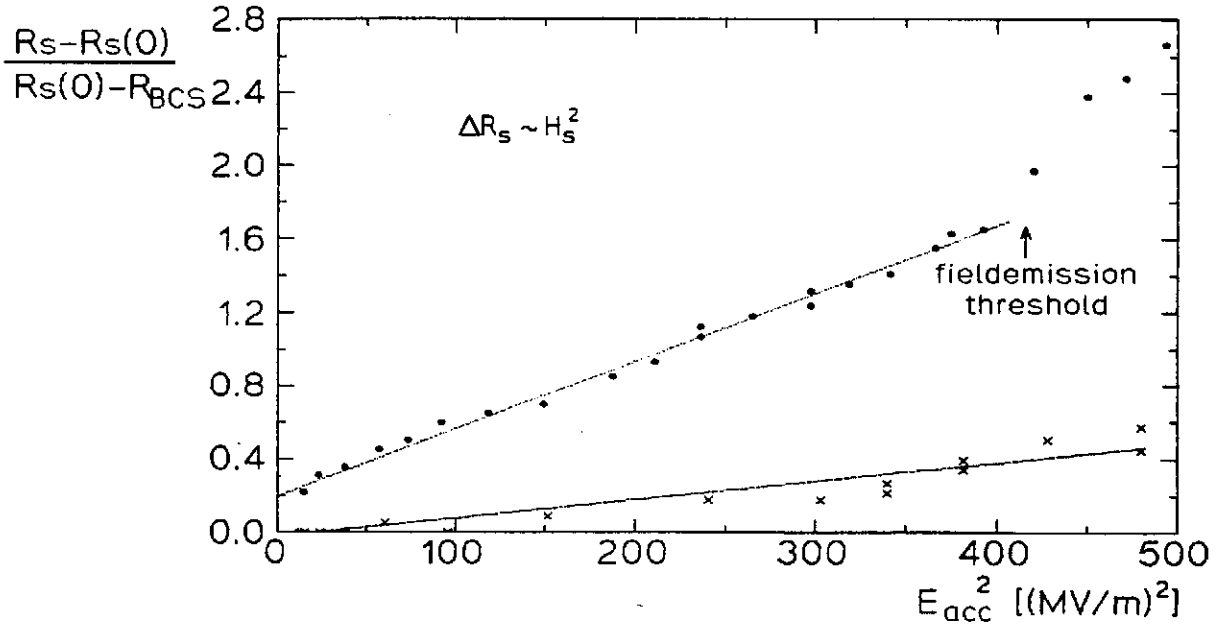

Fig. 6c: Increase of the residual surface resistance ΔR_s with E_{acc}^2

As reported in a former paper [6], both the exponential temperature increase on the defect and the increase of R_S with H_S^2 cannot be described by thermal model calculations assuming a normalconducting defect with constant $R_{s,def}$. As a first step curing this lack of understanding, eq.(3) was extended by a temperature dependence of the surface resistance of the local defect. Furthermore, as mentioned above, one could imagine, that the presence of the thermometer leads to a drastically reduced local heat transfer to the helium bath, which may result in the observed exponential temperature increase due to the exponential increase of the BCS resistance with temperature. A new series of model calculations using these ideas are underway.

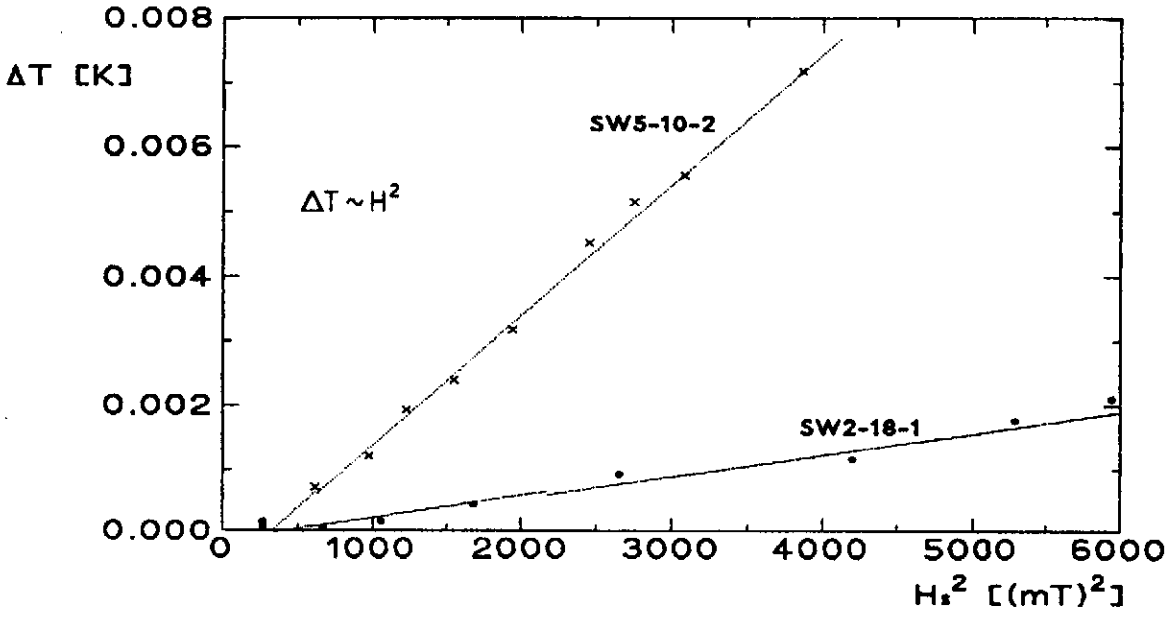

Fig.7: Measured temperature increase ΔT versus H_S^2 at a defect-free area of the cavity wall

No detected defect

Both analysed experiments were limited by field emission and in the first cryotest no local temperature increase except tat due to the electron bombardement above the field emission threshold was observed. The residual Q_0-values were more than a factor of 2 higher than in the above described experiments (SW5-10-2: $Q_0 = 2.2 \cdot 10^{10}$; SW2-21-1: $Q_0 = 2.5 \cdot 10^{10}$). Analysing the temperature increase at the defect-free area at the equator with respect to the local surface resistance (Fig.7), we obtain:

SW2-21-1: $R_s^{loc}(1.38K) = (4-8)n\Omega \quad \leftrightarrow \quad R_{s,res}(RF) = 11.6\ n\Omega \qquad (R_{s,BCS}(1.38K) \approx 2n\Omega)$

SW5-10-1: $R_s^{loc}(1.45K) = (7-10)n\Omega \quad \leftrightarrow \quad R_{s,res}(RF) = 13.2\,n\Omega \qquad (R_{s,BCS}(1.45K) \approx 3.5n\Omega)$

The surface resistance due to frozen-in-flux contributes $R_{s,fif} \leq 4n\Omega$ in addition to the BCS-resistance.

Again most of the cavity surface shows no or only a very small magnetic residual surface resistance. The discrepancy between the integrally measured RF-surface resistance $R_s = G/Q_0$ and the locally obtained value using the temperature increase is in agreement with the model of afew spots or small areas, which contribute significantly to the residual RF-surface resistance. This is supported by the development of the residual Q_0-value during experiment SW5-10. After the first cool-down to 1.4K the cavity showed a Q_0-value of $Q_0 = 7 \cdot 10^{10}$. During field emission and processing of field emission before the final cryotest with fixed thermometers, the Q_0 degraded to $2.2 \cdot 10^{10}$, which obviously can be attributed to the properties of the field emission site.

High residual resistance + areas of increased temperature

As decribed above the "soft" surface treatment with only a HNO_3-soak + ultrapure water rinsing resulted in an increased residual surface resistance of $R_{s,res} = (48-58)n\Omega$ ($\triangleq Q_{0,res} = (5-6) \cdot 10^9$). Temperature maps showed 3 areas of increased losses near the upper iris of the cavity.

For the first time at T = 1.4K, the normally expected temperature increase $\Delta T \sim H^2$ was observed not only at the defect-free cavity surface, but at the lossy area, too. For the analysed area of increased losses, which did <u>not</u> lead to a quench, a surface resistances $R_s^{loc} \geq 90n\Omega$ was obtained. This value represents only a lower limit of the local residual resistance, because the calibration of η for the corresponding thermometer is based on the assumption of a low $R_{s,BCS}(T)$ only. At the defect-free cavity surface a residual surface resistance of at least $R_s^{loc} = 12\,n\Omega$ up to $R_s^{loc} = 33\,n\Omega$ was observed.

Although during this test a local residual resistance definitely higher than 5nΩ (note the contribution of R_{BCS} and R_{flf}) occured for the first time, a few located areas with increased losses dominate the surface resistance of the cavity again.

CONCLUSION

Our test series on high purity niobium cavities has shown, that electric and magnetic surface fields corresponding to accelerating gradients > 25MV/m can be obtained reproducibly with standard preparation techniques. Related to this, residual Q_0-values above 10^{10} at low fields are achieved routinely. A chemical treatment with final ultrapure water rinsing and drying with pure nitrogen resulted in the smallest surface resistance of $R_S(1.4K) = 4.1n\Omega$ ($\triangleq Q_0 = 7 \cdot 10^{10}$).

Despite the increased BCS-resistance at 3GHz magnetic surface fields up to 110mT are achieved even at 2K. In agreement with thermal model calculations for frequencies $f_0 \leq 3$GHz and T = 2K, surface fields of about 100mT can be reproducibly obtained with postpurified niobium.

Several effects are identified to cause the residual surface resistance:

The experiments have shown, that hydrocarbon contaminations of the vacuum system are responsible for high residual losses. Thus, a strict requirement is a careful and clean operation of the cavity vacuum as well as a permanent control of the residual gas composition. Despite former measurements elsewhere, no significant influence on the cavity performance after the exposure to various gases is observed. Especially, nitrogen and air, which are used during the preparation procedure, don´t show deteriorative effects.

In several experiments we proved by thermometry, that the observed low residual resistance is mostly caused by one or very few localized areas. In the defect-free areas, i.e. for the majority of the cavity surface, the surface resistance comes very close to the sum of the BCS-contribution and the very small resistance due to frozen-in-flux. It was also confirmed, that local defects or small areas of increased losses are responsible for the increase of R_S with increasing surface field.

Field emission or the processing of field emitters sometimes degrades the cavity performance.

Reassembly, transport and moving of a cavity does neither affect the residual resistance nor the threshold of field emission. The field emission threshold is usually beyond $E_{peak} > 30 MV/m$ for experiments, which are not influenced by hydrocarbon contamination. Comparably low field enhancement factors β between 60 and 90 are observed after He-processing.

ACKNOWLEDGEMENT

We are grateful to Claire Antoine, Bernhard Bonin, Bernhard Mahut and their collegues, who gave us the opportunity and their support to use the preparation and cleanroom facilities at CEN Saclay.

It is a pleasure to thank Larissa Sevryukova, Peter Kneisel and Vladislav Kurakin for the material and the fabrication of the cavities SW5 and SW6.

This work was funded by the German Federal Minister for Research and Technology (BMFT) under the contract number 05 5WT 85 I (7).

REFERENCES

[1] TESLA-Collaboration, TESLA-Report 93-1, DESY (1993)
[2] R.W.Röth, Dissertation, WUB-DIS 92-12, Universität Wuppertal (1993)
[3] W.Diete, Diplomarbeit, WU D 93-13, Universität Wuppertal (1993)
[4] J. Graber, Thesis, Cornell University (1993)
[5] G.Müller, Proc. of "3rd Workshop on RF Superconductivity", ANL-PHY-88-1 Argonne, p.331 (1988)
[6] R.W.Röth et al., Proc. of the 3rd European Part. Acc. Conf. EPAC, Berlin, p.1325 (1992)
[7] R.W.Röth et al., Proc. of the 2nd European Part. Acc. Conf. EPAC, Nice, p.1097 (1990)
[8] Q.S.Shu et al., Nucl. Instr. and Meth. A278, p.329 (1989)
[9] D.W.Reschke et al., this conference
[10] C.Z.Antoine et al., Proc. of "5th Workshop on RF Superconductivity", DESY Report M92-1, Hamburg, p.456 (1991)
[11] R.W.Röth et al., p.599, ibid. [10]
[12] P.B.Wilson et al., IEEE Trans. Nucl. Sci., NS-20, 104 (1973)
[13] Schnitzke et al., Appl.Phys. 5, 77-78 (1974)
[14] H.Padamsee et al., Proc. of "4th Workshop on Rf Superconductivity", KEK, Tsukuba, KEK Report 89-21 (1989)
[15] P.Kneisel et al., IEEE Trans. on Magn. MAG-23, 1417 (1987)
[16] M.Fouaidy et al., p.547 ibid. [10]
[17] F.Zobel, Diplomarbeit, WUD 89-4, Univ.Wuppertal (1989)

Table 2: RF-Results

BCP10: 10µm etching with final ultrapure water rinsing ; HTA: high temperature annealing ; Q: quench (local thermal breakdown) ; FE: field emission ; RT: room temperature ; He-Proc.: Helium-processing with 40W ; N_2-drying: drying with pure, dustfree nitrogen
The onset of field emission is defined as the threshold of 1nA-current at the probe for the transmitted power.

Test	Surface Preparation	Q_0^{max} [10^9]	E_{peak}^{max} [MV/m]	$Q_0(E_{peak}^{max})$ [10^9]	E_{peak}^{onset} [MV/m]	H_s [mT]	E_{acc} [MV/m]	Comments (limitation)
SW1-19	BCP35, HTA	7.0	26.5	3.5	12.8	43.5	10.4	FE
SW1-20	BCP15	35	(45.4)	8.0	38.3	(74.4)	(17.8)	**not** max P_{inc}
SW1-20-1	RT-cycle	26	61.2	1.4	39.8	100.3	24	FE,power
SW1-20-2	RT-cycle, He-gas	18	66.3	2.0	43.9	108.7	26	FE,power,He-Proc.
SW1-20-3	RT-cycle, N_2-gas	24	64.0	2.0	39.5	104.9	25.1	FE,power,He-Proc.
SW1-20-4	RT-cycle, syn.Air	19	(56.1)	7.0	43.4	(92.0)	(22)	FE, **not** max.P_{inc}
SW1-20-5	RT-cycle	14	60.4	3.7	36.0	99.1	23.7	FE,power
SW1-20-6	RT-cycle, CO_2	15	55.9		34.4	91.5	21.9	FE,power
SW2-16	BCP33, HTA	30±20	62.0	1.0	40.8	101.6	24.3	FE,power, $\beta_1 \gg 1$
SW2-17	Re-assembling	30±20	56.1	1.0	38.3	92.0	22.0	FE,power, $\beta_1 \gg 1$
SW2-18	BCP9 (**Saclay**)	9.0	68.9	2.5	66.3	112.9	27.0	Q
SW2-18-1	RT-cycle	9.5	67.6	2.3	>67.6	110.8	26.5	Q
SW2-19	HNO_3, N_2-drying	4.2	54.3	1.2	34.4	89.0	21.3	FE,power,He-Proc.
SW2-20	HNO_3	5.0	53.6	1.3	34.4	87.8	21.0	FE,power,He-Proc.
SW2-20-1	RT-cycle	6.0	55.3	1.4	31.9	90.7	21.7	FE,power
SW2-21	BCP10, N_2-drying (**Saclay**)	35±15	67.1	0.8	41.6	109.9	26.3	FE,power, $\beta_1 \gg 1$
SW2-21-1	RT-cycle	25±5	69.1	0.9	44.4	113.3	27.1	FE,power, $\beta_1 \gg 1$
SW5-9	BCP30, HTA	0.6	17.6	0.4	15.3	28.8	6.9	vacuum accident
SW5-10	BCP15, N_2-drying	70	(61.0)	1.7	39.5	(99.9)	(23.9)	FE, **not** max.P_{inc}
		33	50.0	0.6	31.9	81.9	19.6	decrease due to FE
SW5-10-1	RT-cycle	34	53.8	0.6	34.4	88.2	21.1	FE,power
SW5-10-2	RT-cycle	22	63.8	0.7	32.6	104.5	25.0	FE,power,He-Proc.
SW5-11	BCP10, N_2-drying (**Saclay**)	41	(31.1)	19	25.5	(51)	(12.2)	FE, **not** max. P_{inc}
		6	53.6	0.6	≈33	87.8	21	decrease due to FE
SW6-2	BCP25	4.0	15.8	1.8	>15.8	25.9	6.2	Q